

This is a repository copy of *Recombination of Protons Accelerated by a High Intensity High Contrast Laser*.

White Rose Research Online URL for this paper:

<https://eprints.whiterose.ac.uk/id/eprint/136928/>

Version: Published Version

Article:

Tata, Sheroy, Mondal, Angana, Sarkar, Soubhik et al. (6 more authors) (2018)
Recombination of Protons Accelerated by a High Intensity High Contrast Laser. *Physical Review Letters*. 134801. ISSN: 1079-7114

<https://doi.org/10.1103/PhysRevLett.121.134801>

Reuse

Items deposited in White Rose Research Online are protected by copyright, with all rights reserved unless indicated otherwise. They may be downloaded and/or printed for private study, or other acts as permitted by national copyright laws. The publisher or other rights holders may allow further reproduction and re-use of the full text version. This is indicated by the licence information on the White Rose Research Online record for the item.

Takedown

If you consider content in White Rose Research Online to be in breach of UK law, please notify us by emailing eprints@whiterose.ac.uk including the URL of the record and the reason for the withdrawal request.

Recombination of Protons Accelerated by a High Intensity High Contrast Laser

Sheroy Tata,¹ Angana Mondal,¹ Soubhik Sarkar,¹ Jagannath Jha,¹ Yash Ved,¹ Amit D. Lad,¹
James Colgan,² John Pasley,³ and M. Krishnamurthy^{1,4,*}

¹Tata Institute of Fundamental Research, Mumbai 400 005, India

²Los Alamos National Laboratory, New Mexico 87544, USA

³York Plasma Institute, Department of Physics, University of York, York, YO10 5DD, United Kingdom

⁴TIFR Centre for Interdisciplinary Sciences, Hyderabad 500 075, India



(Received 8 March 2018; published 25 September 2018)

Short pulse, high contrast, intense laser pulses incident onto a solid target are not known to generate fast neutral atoms. Experiments carried out to study the recombination of accelerated protons show a 200 times higher neutralization than expected. Fast neutral atoms can contribute to 80% of the fast particles at 10 keV, falling rapidly for higher energy. Conventional charge transfer and electron-ion recombination in a high density plasma plume near the target is unable to explain the neutralization. We present a model based on the copropagation of electrons and ions wherein recombination far away from the target surface accounts for the experimental measurements. A novel experimental verification of the model is also presented. This study provides insights into the closely linked dynamics of ions and electrons by which neutral atom formation is enhanced.

DOI: 10.1103/PhysRevLett.121.134801

Diagnostic neutral particle beams are at the forefront to probe Tokamak plasmas and directed heating in fusion plasmas [1,2]. Energetic neutral atoms found in the early Universe are important from an astrophysical perspective [3]. Neutral atom beam formation in intense laser plasmas is a less explored perspective. Understanding charge transfer dynamics of neutral beam formation in laser plasmas is important both for fundamental and applied sciences.

Intense ultrashort pulses emit a high current of hot electrons instantly from the target before the ions move. The instantaneous electrostatic field can be as large as MV/ μ m. Target atoms are ionized and accelerated by this target normal sheath acceleration (TNSA) field, as schematically shown in Fig. 1(a). Lighter protons move out fastest from the target surface and are thus seen from all targets, as they are present as a surface contaminant. Such microsized accelerators form megaelectron ion beams and have attracted significant attention [4,5]. Major studies focused on increasing ion energy, reducing beam emittance, and promoting novel applications [6–9]. But in all the years of work on ion acceleration with ultrashort pulse, intense, high contrast laser pulses, accelerated fast neutral atom generation has not been observed. With 30 fs laser pulses focused to 10^{18} W/cm², the plasma temperature peaks to ≈ 20 keV and at most 0.2% charge neutralization is expected [see Fig. 1(b)]. On the other hand, novel experimental methodology adapted here shows about 200 times higher neutralization and fast H atoms up to 60 keV. Invoking all the charge reduction reactions that form neutrals and detailed modeling shows that none of the conventional processes account for the observed

neutralization. To explain this discrepancy, a new scheme that relies on copropagation of ions and electrons is invoked to reproduce the measured H spectrum. Low energy electrons that are also ejected from the target are attributed to causing neutralization. This provides insights into neutral atom generation that have not been hitherto considered.

Fast neutral atom generation is possible in long pulse experiments due to low temperature electrons [10] or in

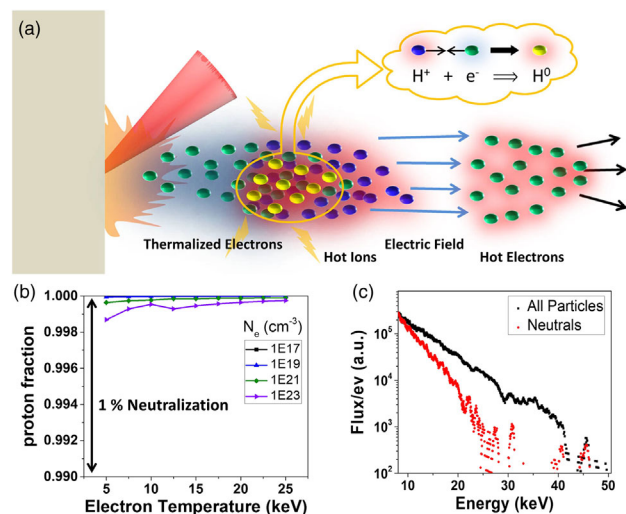


FIG. 1. (a) Model of ion acceleration and neutralization of the fast ions with a cold bunch of copropagating electrons. (b) Steady state average charge of protons in a plasma formed near the target. (c) Spectrum of all particles (H^+ and H atoms) and fast H atoms (neutrals) retrieved from the TOF.

experiments that have a sufficient density of neutral atoms in the neighborhood where the more favorable charge transfer neutralization is possible [11,12]. The high temperature and high density plasma created on solids by an intense, femtosecond, high contrast laser is in a regime that does not allow such charge reduction processes. So, the conditions presented here provide a unique perspective to intense laser plasma interaction, opening insights into hitherto unexplored atomic recombination processes involving closely linked dynamics of electrons and ions.

Experiments here use a 800 nm, 30 fs laser focused on a solid target at 45° to 5×10^{18} W/cm² peak intensity in a 5×10^{-5} mbar vacuum chamber. An intensity contrast $\geq 10^9$ ensures that no significant low temperature pre-plasma is formed to neutralize the accelerated ions. A gated Thomson parabola spectrometer (TPS) is devised to measure both ion and fast atom spectra [13]. A micro-channel plate imaging detector in TPS is time gated to selectively identify the arrival time of only protons and hydrogen atoms. An ungated TPS measurement showed no other ions with a mass-to-charge ratio close to the protons, so an unambiguous signal due to H^+ and H is identified.

A time-of-flight (TOF) measurement to study the neutralization of H^+ is done using two successive data sets (see Supplemental Material [14]). In the first set, all the particles (protons and hydrogen atoms) reach the detector when electric or magnetic fields are not applied to the TPS. This spectrum is shown in black points in Fig. 1(c). In the second set, protons are deflected away from the detector by the application of a strong magnetic field. The spectrum of fast H atoms is shown by the red points in Fig. 1(c). Ratio of the H and $(H + H^+)$ gives the neutralization fraction shown by the red solid line in Fig. 2.

The HYADES code [15] is used to compute the electron density and temperature required to compute neutralization. Electron temperature peaks at ≈ 20 keV and decreases to ≈ 1 keV during the ion acceleration period (see Fig. S2 of the Supplemental Material [14]). To obtain an upper limit of neutralization, steady state calculations are done using FLYCHK [16] with temperature and density ranging all the possible parameter space encompassing HYADES calculations and the results are shown in Fig. 1(b). At most 0.2% neutralization is predicted for our experimental conditions. Any discernible neutralization is feasible only when the electron temperature is less than 2 eV (see Fig. S3(a) of the Supplemental Material [14]). Under our experimental conditions the plasma temperature is 10^2 – 10^4 times higher than 2 eV. On the other hand, copious H atom formation is clearly observed and the neutralization fraction as a function of energy is shown by the solid lines in Fig. 2 for two different targets at different laser intensities and contrasts. To explain these results, we investigate various processes that can lead to fast H atoms. Neutralization by charge transfer with an ambient background is only one tenth of the neutralization measured (see Fig. S1 of the

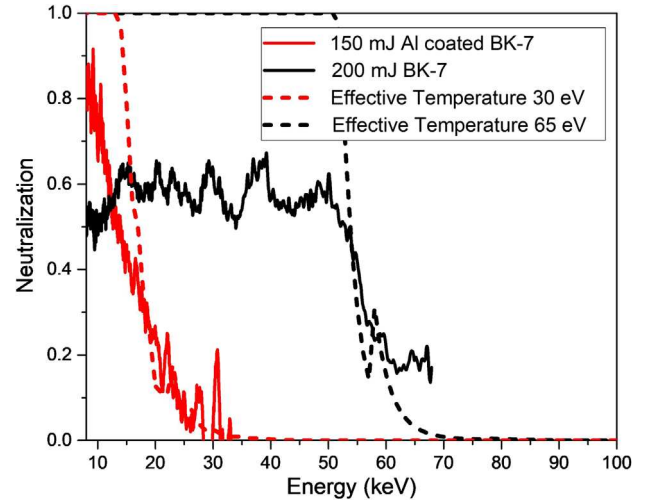


FIG. 2. Neutralization as a function of energy at different experimental conditions. The dashed lines shows neutralization spectrum obtained with the copropagation model.

Supplemental Material [14]). The decrease in neutralization with energy due to charge transfer is more gradual than the observations. Thus, this mechanism cannot explain the observed fast H atom generation.

Charge transfer with atoms released from the target surface could be proposed as another possible mechanism. In the case of long pulse experiments [10,12] or short pulses with poor contrast, ions pass across the plume having neutral atoms and undergo neutralization by charge transfer. In experiments with extended targets such as clusters [11], liquid sprays [12,17] both charge transfer with neutral atoms and/or Rydberg excited systems near the laser focus contribute to neutralization. The use of a high contrast laser provides a cleaner interaction with the solid target in our experiments. A HYADES calculation shows that the average charge state of Al ions in the plasma plume is 13, and so all the atoms at the target front are fully stripped (see Figs. S2(b) and S2(c) of the Supplemental Material [14]). The absence of neutral atoms at the target front therefore rules out charge transfer contributing to the observed neutralization. Any ablative emission of neutral atoms will be long after the protons leave the plasma from the target front and the protons that are ahead of the heavier atoms would not undergo charge transfer. Also, during the period that the protons are close to the target, the static fields are expected to be high and can lead to strong auto-ionization. Thus, fast atoms are not expected to come from the target surface or be formed by charge transfer near the target front. We also note that the measured neutralization energy spectrum differs very much from the curve predicted by charge transfer (see Fig. S1 of the Supplemental Material [14]).

All these considerations prompted us to understand charge neutralization via electron-ion recombination. Three major processes of electron-ion recombination are

dielectronic recombination, three body recombination, and radiative recombination [18]. Computation of the electron-ion recombination rate, when the ions pass through the plasma plume [electron density as computed in Fig. S3(c) of the Supplemental Material [14]] shows that neutralization is effective only when electron temperatures are ≤ 2 eV. Since the plasma temperature is substantially larger, these processes cannot explain observed neutralization as shown in Fig. 1(b). A mere reduction of the plasma temperature does not explain the neutralization spectrum as seen in Fig. S3(b) of the Supplemental Material [14]. In view of these considerations, we are forced to invoke interactions that occur far away from the target surface and propose a new formalism for fast atom generation. Given that there is a large spread in the electron and ion velocities, it is conceivable that electrons with appropriate velocity copropagate with the ions. Copropagation would reduce the effective electron temperature in the ion reference frame and increases electron-ion interaction time and length. This contributes to more electron-ion recombination and fast neutral atom generation.

An experimental test of the model is devised by imaging the position of the source of H^+ and H^0 under the presence of

an externally applied magnetic field, transverse to the target normal. A schematic of the experiment is shown in Fig. 3(a). The TPS, with certain limitations, also functions as a spatially resolving imaging spectrometer indicating the source of the accelerated particles [19]. An external magnet placed a few mm away from the target would shift the ion trajectory and if neutralization is to occur far away from the target, it would appear as a shift in the origin of the particles in the TPS. The shift in the origin of the neutral species can only be explained based on the change in the position of the virtual source when the initially charged particle deflects in the externally applied magnetic field after which the particle may be converted into a fast neutral atom and drift towards the detector. Figure 3(b) shows the neutral H^0 signal, under approximately 1:1 pinhole imaging conditions, without an external magnetic field. In the presence of the magnetic field, the central spot shifts in the direction of ion deflection by the field, as shown by an arrow in Fig. 3(c). By moving a magnet (4.8 kG surface field) in and out of the plane away from the target in the X direction, the magnetic field is changed along the ion path and a clear drift in the neutral atom spot, shown by the line projection in Fig. 3(d). When the magnet is very far (100 mm from the ion flight

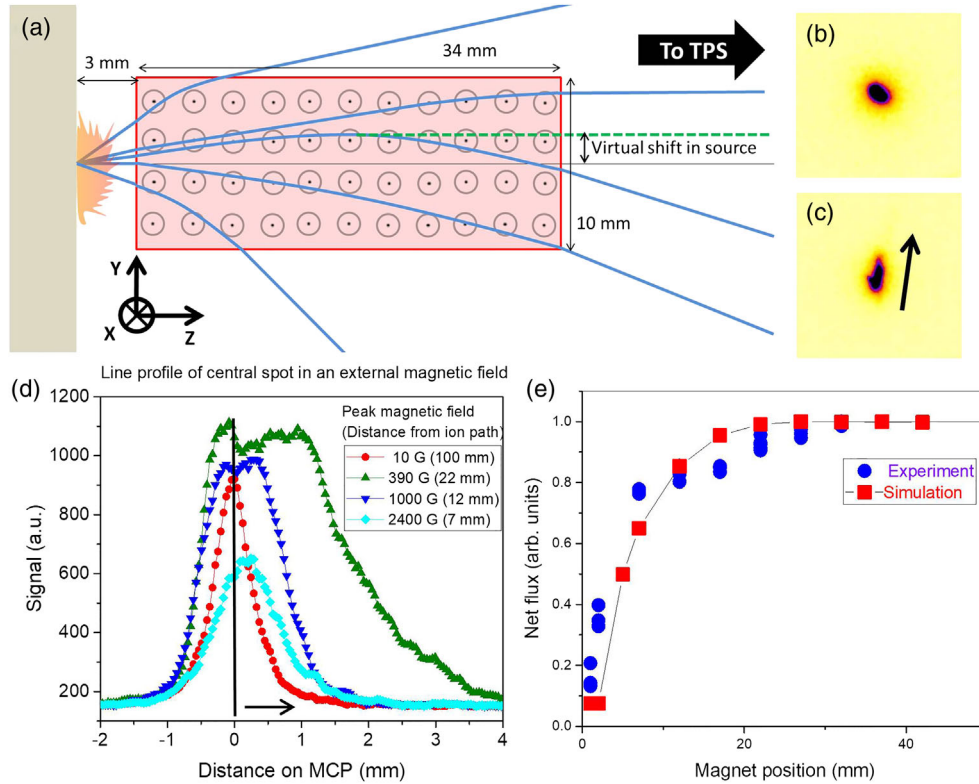


FIG. 3. (a) A schematic of the ion trajectory in the presence of an external magnetic field. The blue and the green (dashed) lines represent the ions and neutral particle trajectories in the field. (b),(c) The central spot of the TPS gated to detect H atoms, without and with a magnetic field, respectively. Change in the shape of the H atom spot indicates a shift in the virtual source position. (d) Line profile in the direction of deflection upon scanning the transverse magnetic field in the x direction. (e) Change in the neutral flux due to the magnetic field applied near the target. The experimental measurements compare well with particle trajectory calculations computed using the pinhole imaging formalism.

path), the central spot is closer to a Gaussian distribution with no apparent drift. As the magnet is brought closer, the distribution starts widening. In this case some of the particles are converted to neutral atoms before the end of the field and the remaining neutrals are formed beyond the magnetic field region resulting in a double hump structure. In case of a larger field (e.g., magnet at 7 mm from target normal), all the neutral atoms are formed before the end of the magnetic field, resulting in a shift in peak position [Fig. 3(d), cyan diamond]. This systematic shift in the virtual source of neutral atoms provides clear evidence of neutralization occurring a few tens of millimeters away from the target and supports the copropagation model. Particle trajectory calculations are done to model the spread of the neutral atom spot seen by the pinhole imaging with the applied magnetic field (see Supplemental Material [14]). The change in proton flux, measured at the detector, due to the applied field is simulated. The position of neutralization is varied along the ion path for a given magnetic field, ensuring that the experimental ratio of the proton to neutral atom flux is conserved. An experimentally observed change in neutral flux is simulated and compared with the experiments in Fig. 3(e). The correlation seen in Fig. 3(e) is a strong experimental evidence in support of the copropagation model and proposition of neutralization occurring far away from the target.

To compute the neutralization by the copropagation model, the calculated electron density was extrapolated up to a few 100 μm from the target surface (see Fig. S2(a) of the Supplemental Material [14]). The electron temperature is much larger and the electrons of such high temperature would be far ahead of the ions and would not contribute to the neutralization. It could be thought that the bulk temperature of the electrons, which is a few hundred electron volts [20] could be used to calculate the neutralization. A 100 eV temperature is too high to cause the neutralization of fast ions and gives neutralization curves that do not correlate with the measurements. The difficulty is actually in assuming that the electrons of a particular temperature should start around the same time as the ions and that the low electron velocity fraction interacts with the ions. Clearly in any real solid target plasma, low energy electrons (< 50 eV) can be released from the target long after the laser pulse or after ions are accelerated from the target. In TNSA, initially fast electrons are ejected and capacitorlike fields accelerate the ions from the surface. After a while, when the ions start moving, the effective potential of the target is reduced and this promotes the escape of low energy electrons from the target. The delayed low energy electrons (effectively tens of electron volts) can copropagate with the ions and take part in neutralization. The density and the temperature of these low energy electrons depends on the dynamics of the number of ions that escape the target. The escaping ion distribution controls the temporal dynamics of the electrostatic potential of the target. Understanding the exact dynamics of

convoluting the time and velocity of the electrons that copropagate with the ions is not a trivial exercise by any means. It is possible to conceive an effective temperature for the electrons which copropagate with the ions. For a particular ion velocity in the spectrum, effective rate coefficients for recombination are used at an effective temperature given by the one dimensional velocity difference between the electron cloud and the ion. Calculation of the fraction of ions converted into neutral particles as they copropagate with the electron cloud is carried out using electron-ion recombination rates at the reduced effective temperature. Neutralization as a function of ion energy is obtained by extending calculations to different ion energies. An iterative scheme is used to obtain an effective temperature at which the functional form of neutralization correlates to experiments, as seen in Fig. 2. A fit to the neutralization spectrum under two different conditions is shown by variation of the effective temperature. In our laboratory, many experiments have been performed using Doppler spectroscopy and pump-probe reflectivity to measure the plasma expansion speed as a function of time at the target front. These experiments [20–25] give cold electron temperatures comparable to the temperatures given by the model in Fig. 2.

The low energy electron emission in reality would be over a broader angular distribution. A transverse expansion of the electrons would lead to reionization of the H atoms by the electrons that are not collinear with the protons. The discrepancy in the simulated neutralization fraction at lower energies is attributed to limitations in the model of using a one dimensional linear velocity component for the low energy electrons. The addition of these features would require parameters to describe the angular dependence of the electrons with velocity and also the electronic states of the H atom formed. While using a larger number of parameters could fit the data, such an exercise does not necessarily provide more information than the experimental demonstration of the copropagation model already discussed.

In conclusion, the formation of fast neutral atoms in high contrast high intense laser produced plasmas is unexpected. Higher electron temperatures and large electrostatic fields elude conventional ion charge reduction close to the target. Careful experimentation reveals that even with high contrast high intensity pulses a much larger fraction of ions is neutralized than anticipated. If one considers the electrons copropagating with the ions, the relative velocity and thus the effective temperature is lower and the path length for the neutralization is larger. This drastically increases the effective recombination rate and the total number of recombination collisions by the enhanced path length or interaction time. Electron copropagation for neutralization far from the solid target has not been discussed in the contemporary literature. The scheme is unambiguously proved experimentally and the computations formulated in this model account for the experimentally measured

neutralization. This scheme should be important in studies that focus on the detailed analysis of charge spectral measurements from the solid target. This could also be a subtle probe of the electron-ion oscillations that have not been observed before. Specific tuning to reduce the electron density should provide a scale of these oscillations and obtaining quasimonoenergetic neutral atoms.

M.K. acknowledges support from the Department of Atomic Energy–Science Research Council outstanding investigator Award.

*mkrisim@tifr.res.in

- [1] M. Murakami, R. C. Isler, J. F. Lyon, C. E. Bush, L. A. Berry, J. L. Dunlap, G. R. Dyer, P. H. Edmonds, P. W. King, and D. H. McNeill, Electron Heating by Neutral-Beam Injection in the Oak Ridge Tokamak, *Phys. Rev. Lett.* **39**, 615 (1977).
- [2] R. C. Isler, An overview of charge-exchange spectroscopy as a plasma diagnostic, *Plasma Phys. Controlled Fusion* **36**, 171 (1994).
- [3] M. Holmstrom, A. Ekenbeck, F. Selsis, T. Penz, H. Lammer, and P. Wurz, Energetic neutral atoms as the explanation for the high-velocity hydrogen around HD 209458b, *Nature (London)* **451**, 970 (2008).
- [4] *Laser-Plasma Interactions and Applications*, edited by P. McKenna *et al.*, Scottish Graduate Series (Springer, Heidelberg, 2013), and references therein.
- [5] M. Roth, Review on the current status and prospects of fast ignition in fusion targets driven by intense, laser generated proton beams, *Plasma Phys. Controlled Fusion* **51**, 014004 (2009).
- [6] E. L. Clark, K. Krushelnick, J. R. Davies, M. Zepf, M. Tatarakis, F. N. Beg, A. Machacek, P. A. Norreys, M. I. K. Santala, I. Watts, and A. E. Dangor, Measurements of Energetic Proton Transport through Magnetized Plasma from Intense Laser Interactions with Solids, *Phys. Rev. Lett.* **84**, 670 (2000).
- [7] F. Fiuza, A. Stockem, E. Boella, R. A. Fonseca, L. O. Silva, D. Haberberger, S. Tochitsky, C. Gong, W. B. Mori, and C. Joshi, Laser-Driven Shock Acceleration of Monoenergetic Ion Beams, *Phys. Rev. Lett.* **109**, 215001 (2012).
- [8] A. Macchi, F. Cattani, T. V. Liseykina, and F. Cornolti, Laser Acceleration of Ion Bunches at the Front Surface of Overdense Plasmas, *Phys. Rev. Lett.* **94**, 165003 (2005).
- [9] A. Macchi, M. Borghesi, and M. Passoni, Ion acceleration by superintense laser-plasma interaction, *Rev. Mod. Phys.* **85**, 751 (2013).
- [10] S. Bagchi, M. Tayyab, B. Ramakrishna, A. Upadhyay, T. Mandal, J. A. Chakera, P. A. Naik, and P. D. Gupta, Micrometer-sized negative-ion accelerator based on ultra-short laser pulse interaction with transparent solids, *Phys. Rev. E* **92**, 051103 (2015).
- [11] R. Rajeev, M. Trivikram, K. P. M. Rishad, V. Narayanan, E. Krishnakumar, and M. Krishnamurthy, A compact laser-driven plasma accelerator for megaelectronvolt-energy neutral atoms, *Nat. Phys.* **9**, 185 (2013).
- [12] F. M. L. Antonelli, A. Flacco, J. Braenzel, B. Vauzour, G. Folpini, G. Birindelli, M. Schnuerer, D. Batani, and V. Malka, Efficient laser production of energetic neutral beams, *Plasma Phys. Controlled Fusion* **58**, 034016 (2016).
- [13] S. Tata, A. Mondal, S. Sarkar, A. D. Lad, and M. Krishnamurthy, A gated Thomson parabola spectrometer for improved ion and neutral atom measurements in intense laser produced plasmas, *Rev. Sci. Instrum.* **88**, 083305 (2017).
- [14] See Supplemental Material at <http://link.aps.org/supplemental/10.1103/PhysRevLett.121.134801> for more details.
- [15] J. T. Larsen and S. M. Lane, HYADES—A plasma hydrodynamics code for dense plasma studies, *J. Quantum Spectrosc. Radiat. Trans.* **51**, 179 (1994).
- [16] H.-K. Chung, M. H. Chen, W. L. Morgan, Y. Ralchenko, and R. W. Lee, FLYCHK: Generalized population kinetics and spectral model for rapid spectroscopic analysis for all elements, *High Energy Density Phys.* **1**, 3 (2005).
- [17] S. Ter-Avetisyan, B. Ramakrishna, M. Borghesi, D. Doria, M. Zepf, G. Sarri, L. Ehrentraut, A. Andreev, P. V. Nickles, S. Steinke, W. Sandner, M. Schnerer, and V. Tikhonchuk, MeV negative ion generation from ultra-intense laser interaction with a water spray, *Appl. Phys. Lett.* **99**, 051501 (2011).
- [18] Y. Hahn, Electron-ion recombination processes—An overview, *Rep. Prog. Phys.* **60**, 691 (1997).
- [19] R. Rajeev, K. P. M. Rishad, T. Madhu Trivikram, V. Narayanan, and M. Krishnamurthy, A Thomson parabola ion imaging spectrometer designed to probe relativistic intensity ionization dynamics of nanoclusters, *Rev. Sci. Instrum.* **82**, 083303 (2011).
- [20] V. M. Gordienko, I. M. Lachko, P. M. Mikheev, A. B. Savel'ev, D. S. Uryupina, and R. V. Volkov, Experimental characterization of hot electron production under femto-second laser plasma interaction at moderate intensities, *Plasma Phys. Controlled Fusion* **44**, 2555 (2002).
- [21] S. Mondal, A. D. Lad, S. Ahmed, V. Narayanan, J. Pasley, P. P. Rajeev, A. P. L. Robinson, and G. R. Kumar, Doppler Spectrometry for Ultrafast Temporal Mapping of Density Dynamics in Laser-Induced Plasmas, *Phys. Rev. Lett.* **105**, 105002 (2010).
- [22] A. Adak, A. P. L. Robinson, P. K. Singh, G. Chatterjee, A. D. Lad, J. Pasley, and G. R. Kumar, Terahertz Acoustics in Hot Dense Laser Plasmas, *Phys. Rev. Lett.* **114**, 115001 (2015).
- [23] A. Adak, P. K. Singh, D. R. Blackman, A. D. Lad, G. Chatterjee, J. Pasley, A. P. L. Robinson, and G. R. Kumar, Controlling femtosecond-laser-driven shock-waves in hot, dense plasma, *Phys. Plasmas* **24**, 072702 (2017).
- [24] P. K. Singh, G. Chatterjee, A. Adak, Amit D. Lad, P. Brijesh, and G. Ravindra Kumar, Ultrafast optics of solid density plasma using multicolor probes, *Opt. Express* **22**, 22320 (2014).
- [25] M. Dalui, T. M. Trivikram, J. Colgan, J. Pasley, and M. Krishnamurthy, Compact acceleration of energetic neutral atoms using high intensity laser-solid interaction, *Sci. Rep.* **7**, 3871 (2017).